Compact Wavelength Demultiplexer via Photonic Crystal Multimode Resonators

Zhen Hu[1,*] and Ya Yan Lu[2]

[1]*Department of Mathematics, Hohai University, Nanjing, Jiangsu, China*
[2]*Department of Mathematics, City University of Hong Kong, Kowloon, Hong Kong*

[*]*Corresponding author: huzhen1230@gmail.com*

Wavelength demultiplexers based on photonic crystal resonators are attractive, since they may be realized in very small sizes. However, existing designs have a limitation on the size, since they all require one resonator for each wavelength and these resonators must be separated. As a possible approach to reduce the size further, we show that a single multimode resonator may be used to separate different wavelengths corresponding to the different resonant frequencies. Specifically, we propose an ultra-compact three-wavelength demultiplexer based on a single multimode resonator in a photonic crystal. The design is obtained by an efficient optimization procedure, and its property is analyzed rigorously by a numerical method, as well as approximately by the temporal coupled mode theory.

OCIS codes:

1. Introduction

In optical communication systems, a compact wavelength demultiplexer that separates light with different frequencies is essential [1, 2]. Photonic crystals (PhCs) [3] have the potential to provide ultra-compact components and devices for integrated photonics and other applications. A number of wavelength division multiplexing (WDM) systems based on PhCs have been proposed and realized in experiments. These PhC WDM systems are developed based on resonators [4–15], waveguide couplers [16–18], or superprism effects [19–21]. Those based on PhC resonators are particularly attractive due to their small sizes. Currently, all existing designs based on PhC resonators require one resonator for each frequency. For example, the four-port channel drop filter of Fan *et al.* [4] contains two microcavities supporting two degenerate modes at the desired frequencies. The three-port designs given in [6, 9–11, 14] include one resonator in front of each output waveguide. In the device of Liu *et al* [15], each

output waveguide is connected to a point-defect microcavity, and these microcavities are further connected to a common coupling region.

In this paper, we show that a properly designed multimode resonator can be used as an ultra-compact wavelength demultiplexer. Specifically, we propose a three-frequency wavelength demultiplexer based on a four-port multimode resonator in a square-lattice PhC. The resonator is connected by four semi-infinite PhC waveguides, where one waveguide serves as the input port and the other three serve as the output ports. It has three resonant modes corresponding to three different frequencies. At each of these three frequencies, light propagates to one of the three output waveguides with little reflection and little cross talk. Compared with the existing designs where each frequency requires a resonator, the size of our demultiplexer is much smaller.

2. Wavelength demultiplexer

Our proposed wavelength demultiplexer is shown in Fig. 1, where the background PhC is a

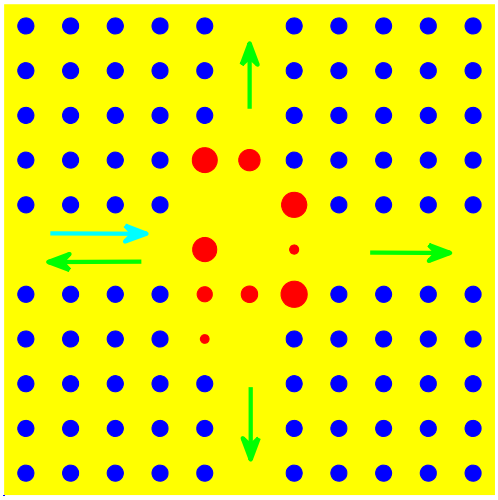

Fig. 1. Three-frequency wavelength demultiplexer in a square-lattice photonic crystal.

square lattice of dielectric rods surrounded by air. The refractive index and the radius of the rods are 3.4 and $0.18a$ respectively, where a is the lattice constant. The semi-infinite PhC waveguides are obtained by removing a row of rods. The structure is considered for the E polarization, for which the electric field is parallel to the axes of the rods. The PhC has a bandgap given by $0.302 < \omega a/(2\pi c) < 0.443$, and the PhC waveguide has a single guided mode for $0.312 < \omega a/(2\pi c) < 0.443$, where ω is the angular frequency and c is the speed of light in vacuum. The area around the center of the structure is regarded as a resonator and

it contains nine rods (shown in red in Fig. 1) with different radii and the same refractive index as the original rods. If we order the nine rods by columns from left to right and in each column from bottom to top, the radii of these rods are $0.0970a$, $0.1688a$, $0.2698a$, $0.2793a$, $0.1843a$, $0.2389a$, $0.2939a$, $0.1024a$ and $0.2823a$, respectively. The structure is designed to separate three frequencies corresponding to $\omega_1 = 0.36$, $\omega_2 = 0.37$ and $\omega_3 = 0.38$ $(2\pi c/a)$. The left-horizontal waveguide is the input port. The right-horizontal, the lower-vertical and the upper-vertical waveguides are the output ports for ω_1, ω_2 and ω_3, respectively.

The structure is found by solving an optimization problem where the radii of selected rods in the central area are the free parameters. The refractive indices of the rods are unchanged and their positions are fixed at the lattice points. The optimization problem is to maximize $T_1(\omega_1) + T_2(\omega_2) + T_3(\omega_3)$, where T_1, T_2 and T_3 are relative powers transmitted to the right-horizontal, lower-vertical and upper-vertical semi-infinite waveguides, respectively. The problem is solved by the BFGS quasi-Newton method [22]. In each iteration, the Dirichlet-to-Neumann (DtN) map method developed in our earlier works [23–25] is used to calculate the transmission coefficients for the three frequencies. That method can take advantage of the many identical unit cells and the circular geometry of the rods, and it includes a rigorous boundary condition for terminating PhC waveguides [23]. As a result, our problem can be simulated in a computational domain that contains only 11×11 unit cells. As shown in Fig. 1, the optimized structure contains a few empty unit cells for which the radius of the rod is zero. For simplicity, we have assumed a constant refractive index for the dielectric rods at the three frequencies. Our method can easily take care of material dispersion, since the transmission coefficients for the three frequencies are calculated separately.

The transmission spectra for the three output waveguides are shown in Fig. 2(a). The total power transmitted to the three output waveguides and the reflected power in the input waveguide are shown in Fig. 2(b). In particular, we have $T_1(\omega_1) = 0.9453$, $T_2(\omega_2) = 0.9327$ and $T_3(\omega_3) = 0.9447$. The electric field patterns (the real part of E_z) at the three target frequencies are shown in Fig. 3 (the three images to the left). For all three cases, we observe that the field has nearly the same magnitude in the input (left-horizontal) waveguide and in one output waveguide, and it has a very small magnitude in the other two output waveguides. There is also a strong field somewhere around the center of the structure indicating a link with resonances.

Notice that our demultiplexer (involving nine dielectric rods of different radii) is contained in a rectangular region covering 3×5 unit cells. This is even smaller than the three-wavelength demultiplexer developed in [15] which requires a coupling region of 4×15 unit cells. The structure is designed with three output waveguides pointing to different directions. If parallel output waveguides are desired, they can be easily connected by high performance 90° bends [26].

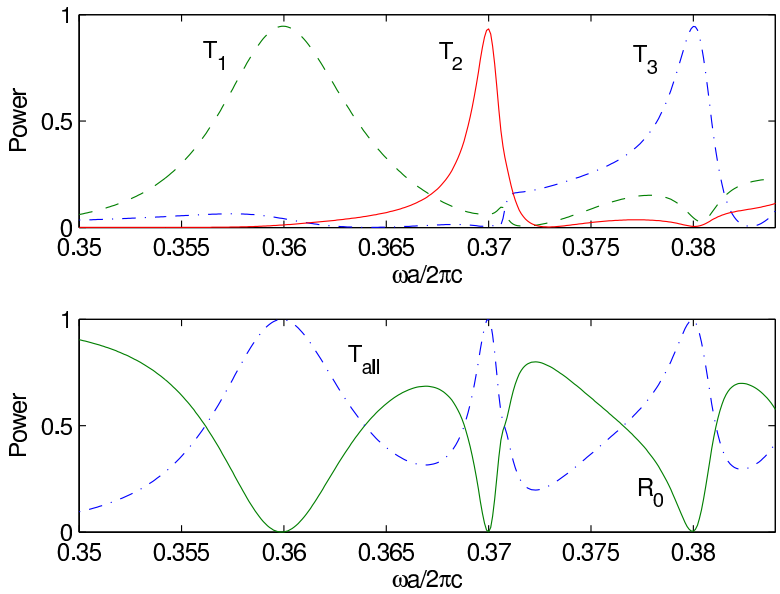

Fig. 2. (a) Normalized transmitted powers in the three output waveguides. (b) Total normalized transmitted power in the output waveguides and the reflected power in the input waveguide.

3. Resonant modes

The phenomenon that incident light from the input waveguide is routed into one of the three output waveguides at each target frequency can be explained by the resonant modes of the structure. While the DtN-map method described in our earlier work [23, 24] solves boundary value problems for a given real frequency, it can also be used to solve eigenvalue problems where the frequency is the unknown [27, 28]. Since power can escape through the waveguides, the resonator has leaky modes with complex frequencies. The DtN-map method developed in [28] is capable of computing leaky modes. In particular, the boundary condition for terminating PhC waveguides has been extended to the complex frequency domain. As a result, we can calculate the leaky modes of our structure in a small truncated domain S, i.e., a square with 11×11 unit cells, using rigorous outgoing radiation boundary conditions on all four sides of S. The method calculates the complex ω iteratively. For any given ω, the DtN-map method gives us a square matrix $\mathbf{A}(\omega)$, and it satisfies

$$\mathbf{A}(\omega)\boldsymbol{u} = 0 \tag{1}$$

if ω is the complex frequency of a leaky mode, where $\boldsymbol{u}$ is a column vector for E_z on the edges of unit cells in the truncated domain S. The length of $\boldsymbol{u}$ is proportional to the number of discretization points N on each edge of the unit cells. Since the interiors of the unit cells

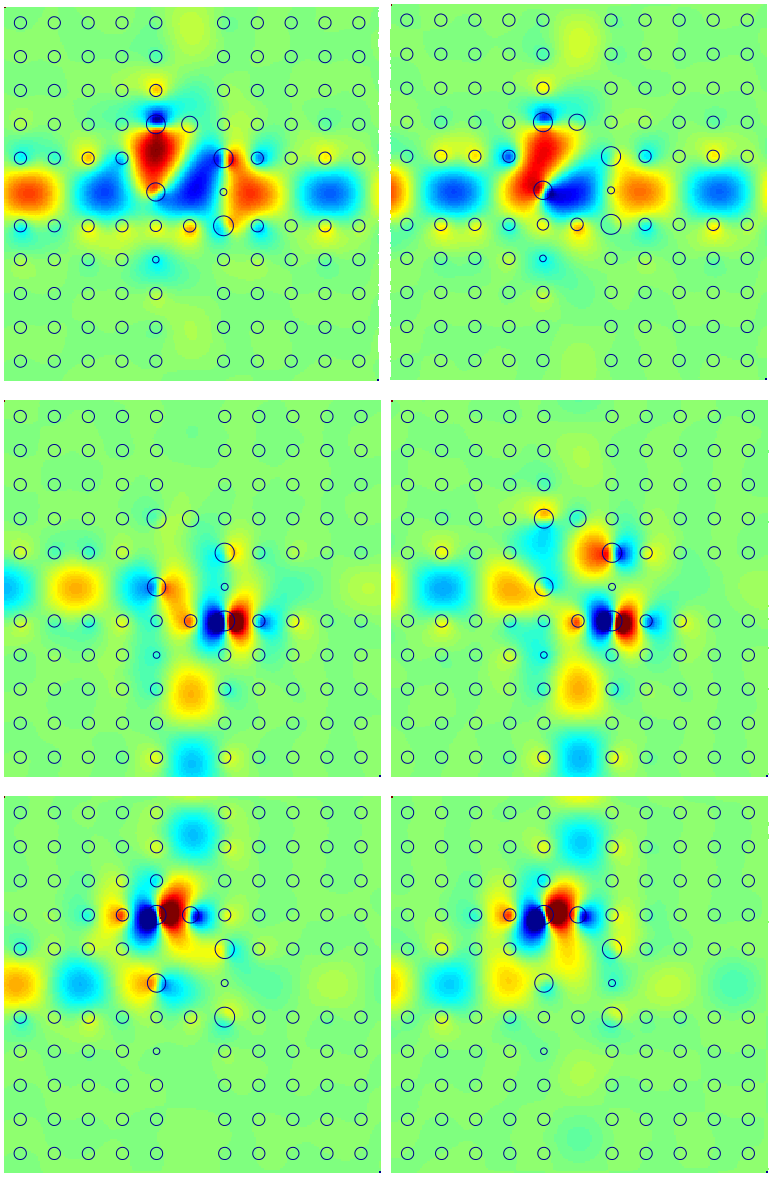

Fig. 3. Left: Electric field patterns for a given incident wave in the left-horizontal waveguide at the three target frequencies. From top to bottom, $\omega a/2\pi c = 0.36,\ \ 0.37,\ \ 0.38$. Right: Electric field patterns of three leaky modes. From top to bottom, $\omega a/2\pi c = 0.35972 - 0.00402i$, $0.37017 - 0.00078i$, $0.38044 - 0.00109i$

are completely avoided, the size of $\mathbf{A}$ is not very large. The leaky modes correspond to those complex ω, such that $\mathbf{A}(\omega)$ is a singular matrix.

To find the leaky modes, we solve ω from $\sigma_1(\mathbf{A}) = 0$, where σ_1 is the smallest singular value of $\mathbf{A}(\omega)$. Initial guesses for the complex roots are provided by real values of ω, where σ_1 reach local minima. Using $N = 7$, we calculate $\sigma_1(A)$ for real frequency ω given by $0.35 \leq \omega a/(2\pi c) \leq 0.39$, and find four local minima around $\omega a/(2\pi c) = 0.36$, 0.37, 0.38 and 0.386. Using these real values as initial guesses, we find the complex eigenfrequencies: $\omega a/2\pi c = 0.35972 - 0.004023i$, $\omega a/2\pi c = 0.37017 - 0.0007824i$, $\omega a/2\pi c = 0.38045 - 0.001093i$ and $\omega a/2\pi c = 0.38589 - 0.00099i$ for the four leaky modes, respectively. The real part of the complex ω gives us the resonant frequency, and the imaginary part of ω is related to the attenuation of the mode and the quality factor $Q = -0.5\mathrm{Re}(\omega)/\mathrm{Im}(\omega)$. Notice that our assumed time dependence is $e^{-i\omega t}$, therefore the imaginary part of the complex frequency of a leaky mode is negative. The quality factors of these four modes are $Q \approx 44.7$, 237, 174 and 195, respectively. The resonant frequencies of the first three modes match the target frequencies very well (with three significant digits). The fourth mode is unexpected but it does not affect the structure as a wavelength demultiplexer.

The electric field patterns of the first three modes are shown in Fig. 3 (the three images to the right). The left and right images in Fig. 3 have some similarities, especially for the second and third modes of which the Q factors are larger.

From the field distribution of a resonant mode, we can calculate the loss to each semi-infinite waveguide. For a single mode waveguide, the loss is related to the coupling coefficient between the resonant mode with the propagating mode of the waveguide. Let the coupling coefficient in the jth waveguide be c_j, where $j = 0$, 1, 2 and 3 denote the left-horizontal, right-horizontal, lower-vertical and upper-vertical waveguides, respectively. If we scale the resonant mode such that $|c_0|^2 + |c_1|^2 + |c_2|^2 + |c_3|^2 = 1$, then the Q factor due to loss in the jth waveguide is $Q_j = Q/|c_j|^2$. Similarly, if we let $\tau = -1/\mathrm{Im}(\omega)$ be the lifetime of the mode, then $1/\tau_j$ is the decay factor due to loss in the jth waveguide, where $\tau_j = \tau/|c_j|^2$. For the resonant mode with the complex eigenfrequency $\omega_l = \omega_{l,r} + i\omega_{l,i}$, the temporal coupled mode theory [29] predicts that

$$T_l(\omega) = \frac{4/(\tau_0\tau_l)}{(\omega - \omega_{l,r})^2 + 1/\tau^2} = \frac{4|c_0|^2|c_l|^2\omega_{l,i}^2}{(\omega - \omega_{l,r})^2 + \omega_{l,i}^2}. \tag{2}$$

In Table 1, we list the squared coupling coefficients for the three modes. In Fig. 4, we show $T_l(\omega)$ for $1 \leq l \leq 3$ based on Eq. (2). Comparing Figs. 2(a) and 4, we can see that the prediction by the coupled mode theory is quite good.

We note that the Q factors of the three resonant modes are quite small and not uniform. This is related to the factor that our optimization procedure only maximizes $T_1(\omega_1) + T_2(\omega_2) + T_3(\omega_3)$ and has no control on the widths of the transmission peaks. While the Q factors may

	mode ω_1	mode ω_2	mode ω_3
$\|c_0\|^2$	0.5464	0.5287	0.4565
$\|c_1\|^2$	0.4221	0.0079	0.0519
$\|c_2\|^2$	0.0034	0.4483	0.0212
$\|c_3\|^2$	0.0281	0.0150	0.4704

Table 1. Squared coupling coefficients of the three resonant modes.

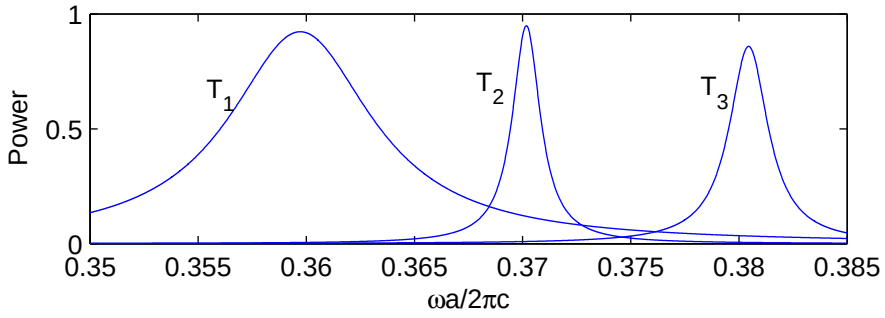

Fig. 4. Transmitted powers to three output waveguides based on the resonant modes and the temporal coupled mode theory.

be increased by enlarging the structure and tuning the entrances of the waveguides, a better optimization formulation is highly desired.

4. Conclusion

In this paper, we show that it is possible to develop ultra-compact wavelength demultiplexers based on multimode resonators in PhCs. We propose a three-wavelength demultiplexer based on a four-port resonator in a square lattice PhC. The resonator has a few resonant modes. Three of them have resonant frequencies corresponding to the three target frequencies of the demultiplexer. Furthermore, these three resonant modes have the desired distribution in their losses to the waveguides. That is, each resonant mode has roughly equal losses in the input and one of the output waveguides, and negligible losses in the other two output waveguides.

Compared with existing designs based on PhC resonators that require one resonator for each wavelength, the size of our demultiplexer is much smaller, since it can be embedded in a rectangular region with only 3×5 unit cells. Our structure is designed for a PhC with a square lattice of infinitely long cylinders, and therefore it has obvious practical limitations.

It is far more useful to develop demultiplexer structures on PhC slabs involving a slab of finite thickness and air-hole arrays, but unfortunately, the design process is extremly time consuming based on existing numerical methods. Nevertheless, it is hoped that our approach based on multimode resonators can be useful in the design of more practical WDM devices.

5. Acknowledgment

This work was partially supported by the National Natural Science Foundation of China under Project 11101122, and the Research Grants Council of Hong Kong Special Administrative Region, China, under Project CityU 102411.

References

1. C. R. Doerr, M. Cappuzzo, L. Gomez, E. Chen, A. Wong-Foy, C. Ho, J. Lam, and K. McGreer, "Planar lightwave circuit eight-channel CWDM multiplexer with <3.9-dB insertion loss," J. Lightw. Technol. **23**(1), 62-65 (2005).
2. J. Xiao, X. Liu, and X. Sun, "Design of an ultracompact MMI wavelength demultiplexer in slot waveguide structures," Opt. Express **15**, 8300-8308 (2007).
3. D. Joannopoulos, S. G. Johnson, J. N. Winn, and R. D. Meade, *Photonic Crystals: Molding the Flow of Light,* 2nd ed. (Princeton University Press, Princeton, NJ, 2008).
4. S. Fan, P. R. Villeneuve, J. D. Joannopoulos, and H. A. Haus, "Channel drop tunneling through localized states," Phys. Rev. Lett. **80**, 960-963 (1998).
5. A. Chutinan, M. Mochizuki, M. Imada, and S. Noda, "Surface-emitting channel drop filters using single defects in two-dimensional photonic crystal slabs," Appl. Phys. Lett. **79**, 2690-2692 (2001).
6. A. Sharkawy, S. Shi, and D. W. Prather, "Multichannel wavelength division multiplexing with photonic crystals," Appl. Opt. **40**(14), 2247-2252 (2001).
7. M. Qiu and B. Jaskorzynska, "Design of a channel drop filter in a two-dimensional triangular photonic crystal," Appl. Phys. Lett. **83**, 1074-1076 (2003)
8. B.-K. Min, J.-E. Kim, and H. Y. Park, "Channel drop filters using resonant tunneling processes in two-dimensional triangular lattice photonic crystal slabs," Opt. Commun. **237**, 59-63 (2004).
9. S. Kim, I. Park, H. Lim, and C.-S. Kee, "Highly efficient photonic crystal-based multichannel drop filters of three-port system with reflection feedback," Opt. Express **12**(22), 5518-5525 (2004).
10. B. S. Song, T. Asano, Y. Akahane, Y. Tanaka, and S. Noda, "Multichannel add/drop filter based on in-plane hetero photonic crystals," J. Lightw. Technol. **23**(3), 1449-1455 (2005).

11. H. Ren, C. Jiang, W. Hu, M. Gao, and J. Wang, "Photonic crystal channel drop filter with a wavelength-selective reflection micro-cavity," Opt. Express **14**(6), 2446-2458 (2006).
12. C.-W. Kuo, C.-F. Chang, M.-H. Chen, S.-Y. Chen, and Y.-D. Wu, "A new approach of planar multi-channel wavelength division multiplexing system using asymmetric super-cell photonic crystal structures," Opt. Express **15**, 198-206 (2007).
13. Y. Kanamori, K. Takahashi, and K. Hane, "An ultrasmall wavelength selective channel drop switch using a nanomechanical photonic crystal nanocavity," Appl. Phys. Lett. **95**(17), 171911 (2009).
14. H. Ren, Y. Qin, H. Wen, Q. Cao, S. Guo, L. Chang, W. Hu, C. Jiang, and Y. Jin, "Photonic crystal three-port channel drop filter based on one-way waveguide," IEEE Photon. Technol. Lett. **24**(5), 332-334 (2012).
15. V. Liu, Y. Jiao, D. A. B. Miller, and S. Fan, "Design methodology for compact photonic-crystal-based wavelength division multiplexers," Opt. Lett. **36**, 591-593 (2011).
16. E. Centeno, B. Guizal, and D. Felbacq, "Multiplexing and demultiplexing with photonic crystals," J. Opt. A: Pure Appl. Opt. **1**, L10-L13 (1999).
17. M. Koshiba, "Wavelength division multiplexing and demultiplexing with photonic crystal waveguide couplers," J. Lightw. Technol. **19**, 1970-1975 (2001).
18. T. Niemi, L. H. Frandsen, K. K. Hede, A. Harpoth, P. I. Bore, and M. Kristensen, "Wavelength-division demultiplexing using photonic crystal waveguides," IEEE Photon. Technol. Lett. **18**(1), 226-228 (2006).
19. H. Kosaka, T. Kawashima, A. Tomita, M. Notomi, T. Tamamura, T. Sato, and S. Kawakamib, "Photonic crystals for micro lightwave circuits using wavelength-dependent angular beam steering," Appl. Phys. Lett. **74**, 1370-1372 (1999).
20. K. B. Chung and S. W. Hong, "Wavelength demultiplexers based on the superprism phenomena in photonic crystals," Appl. Phys. Lett. **81**, 1549-1551 (2002).
21. A. S. Jugessur, A. Bakhtazad, A. G. Kirk, *et al.*, "Compact and integrated 2-D photonic crystal super-prism filter-device for wavelength demultiplexing applications," Opt. Express **14**, 1632-1642 (2006).
22. J. Nocedal and S. J. Wright, *Numerical Optimization,* 2nd ed. (Springer-Verlag, Berlin, New York, 2006).
23. Z. Hu and Y. Y. Lu, "Efficient analysis of photonic crystal devices by Dirichlet-to-Neumann maps," Opt. Express **16**, 17383-17399 (2008).
24. Z. Hu and Y. Y. Lu, "Improved Dirichlet-to-Neumann map method for modeling extended photonic crystal devices," Opt. Quant. Electron. **40**, 921-932 (2008).
25. Z. Hu and Y. Y. Lu, "A simple boundary condition for terminating photonic crystal waveguides," J. Opt. Soc. Am. B **29**(6), 1356-1360 (2012).
26. Z. Hu and Y. Y. Lu, "Improved bends for two-dimensional photonic crystal waveguides,"

Opt. Commun. **284**, 2812-2816 (2011).

27. S. Li and Y. Y. Lu, "Computing photonic crystal defect modes by Dirichlet-to-Neumann maps," Opt. Express **15**, 14454-14466 (2007).
28. S. Li and Y. Y. Lu, "Efficient method for analyzing leaky cavities in two-dimensional photonic crystals," J. Opt. Soc. Am. B **26**, 2427-2433 (2009).
29. H. A. Haus, *Waves and Fields in Optoelectronics*, Chapter 7 (Prentice-Hall, N.J., 1984).